Photodissociation dynamics of acetylacetone: The OH product state distribution

Min-Chul Yoon, Young S. Choi, and Sang Kyu Kim[a)]
Department of Chemistry, Inha University, Inchon 402-751, Republic of Korea

(Received 25 January 1999; accepted 1 April 1999)

Acetylacetone in the supersonic jet, which exists predominantly as an enolic form, is found to give rise to the OH fragment after the $\pi-\pi^*$ transition induced by the UV absorption. The nascent OH product state distributions are determined using a laser-induced fluorescence technique at the excitation wavelengths of 291 and 266 nm. The OH fragment is vibrationally cold, and its rotational state distribution is peaked at $N=3$ or 4 at the pump wavelength of 291 or 266 nm, respectively. No fluorescence from the excited acetylacetone has been observed even in the energy region near the origin, suggesting the ultrafast nonradiative processes of the excited state. From the measured OH product state distributions, the upper bound for the dissociation energy of the acetylacetone is estimated to be 90.3 kcal/mol. The ratios of Λ-doublets and spin–orbit states of the OH fragment are also measured. A slight preference of the OH fragment in the $^2\Pi_{3/2}$ state over the $^2\Pi_{1/2}$ state is observed. The Π^-/Π^+ ratios, determined by the relative intensity ratios of Q and P (or R) lines, are found to be less than unity, suggesting the preferential cleavage of the C–OH bond on the molecular plane probably due to a relatively strong intramolecular hydrogen bonding of the enolic acetylacetone. The prior calculation reproduces the experiment quite well for the OH rotational state distribution at 291 nm, while it does not for that at 266 nm. This suggests that the transition state in the acetylacetone dissociation, at the low energy near threshold, may be completely loosely defined on the potential energy surface which does not have a barrier to recombination, and it becomes tightened as the energy increases above the reaction threshold. © *1999 American Institute of Physics.* [S0021-9606(99)01824-3]

I. INTRODUCTION

Acetylacetone (2,4-pentanedione) has been widely used as a chelating reagent for the preparation of many useful organometallic compounds, and thus its structure and reactivity have been important issues in many fields of science.[1–5] Acetylacetone can exist as two different structural isomers; diketo and enol, and it is well known from much spectroscopic evidence that the relative population of these two structural isomers varies depending on the characteristics of the environment (see below).

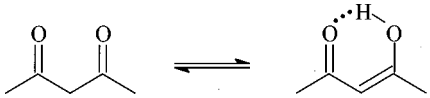

Diketo form Enol form

For example, the diketo form is stable in polar solvents while the enol form is favored in nonpolar solvents.[6,7] In the gas phase at room temperature, acetylacetone is known to exist predominantly as the enol form.[6,7] The preference of the enol form in the gas phase is due to the formation of a relatively strong intramolecular hydrogen bonding in the enolic acetylacetone. The stabilization energy of the hydrogen bonding has been theoretically predicted to be 12 kcal/mol.[8] The molecular structure of the enolic acetylacetone in the ground electronic state has been debated for a long time and seems to remain controversial in terms of whether the hydrogen-bonded H atom is positioned at the center between two adjacent oxygen atoms or not.[9–13] The intramolecular proton transfer dynamics of the enolic acetylacetone have also been intensively studied.[14–17]

Compared to many theoretical and experimental studies on the structure and proton transfer dynamics of acetylacetone, its photochemistry has been given less attention. The UV[7] and electron-impact[18] spectroscopic studies have shown that the enolic acetylacetone in the gas phase at room temperature has a broad structureless absorption band peaked at around 270 nm, which is attributed to the allowed $\pi-\pi^*$ transition. Roubin *et al.* have investigated the photochemistry of acetylacetone in the matrix environment, and have found that the $\pi-\pi^*$ transition is followed by the stereoisomerization of the enolic acetylacetone.[19] Recently, we have reported the first photochemical study of the gas phase acetylacetone.[20] Interestingly, the enolic acetylacetone has found to give the OH and 3-penten-2-on-4-yl radicals in its photodissociation induced by the $\pi-\pi^*$ transition (see below).

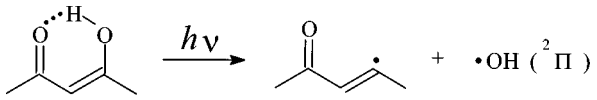

Here, we present a detailed analysis of the quantum state distribution of the OH fragment from the acetylacetone photodissociation.

[a)]Author to whom correspondence should be addressed; electronic mail: skkim@inha.ac.kr

II. EXPERIMENT

Acetylacetone (Aldrich, 99+%) was purchased and used without further purification. Acetylacetone was kept at room temperature and the He carrier gas was bubbled through the sample. The gas mixture was then expanded through a nozzle orifice (General Valve, 0.5 mm diam) into a vacuum chamber with a typical backing pressure of 1 atm. The chamber was equipped with a 6 in. diffusion pump (VHS-6) and a liquid N_2 trap. The background pressure of the chamber was maintained below 10^{-5} Torr when the nozzle (10 Hz) was on. The nozzle was heated to 70 °C to reduce the cluster formation.

The second-harmonic output of a Nd:YAG laser (Spectra-Physics, GCR-150, 10 Hz, 7 ns duration) was split in half and used to pump two independent dye lasers. One dye laser (Lumonics, HD-500) was used to generate the laser pulses in the 580–600 nm range. The output of the dye laser was frequency doubled using a KD*P crystal to generate the UV laser pulses in the 290–300 nm region, and used to excite the molecule (the pump laser pulse). The other dye laser (Lambda Physik, Scanmate II) was used to generate the laser pulses in the 560–580 nm, and its output was frequency doubled to give the laser pulse in the 280–290 nm range. The intensity and direction of the UV output were maintained using a homemade crystal tracking system. This laser pulse (the probe laser pulse) was used to probe the OH fragment from the acetylacetone dissociation. The fourth harmonic output (266 nm) of the Nd:YAG laser was also used for the pump.

The pump and probe laser pulses were combined with a dichroic mirror, directed into the chamber collinearly, and overlapped with a supersonic beam at the position of 20 mm downstream from the nozzle orifice. The delay time between the pump and probe laser pulse was fixed at 10 ns. The polarizations of two pulses were perpendicular to each other, and the polarization of the pump laser was perpendicular to the direction of the fluorescence detection. The laser intensity fluctuation was monitored with a photodiode and used in the normalization of the signal. The laser-induced fluorescence (LIF) signal was detected by a photomultiplier tube (Hamamatsu, H-1949-50), averaged by an integrated boxcar (SRS, SR250), A/D converted by an interface (SRS, SR245), and stored in an IBM personal computer using a data-taking program which also controlled two dye lasers and crystal tracker systems. The intensity of the probe laser was reduced so that the OH transition is not saturated. The linearity of the LIF signal with the probe laser intensity was carefully checked. The LIF signal was averaged for ten shots and the LIF spectra were taken three times at each photolysis wavelength.

III. RESULTS AND DISCUSSION

No fluorescence is observed from the excited acetylacetone even in the wavelength region near the origin of the $\pi-\pi^*$ transition, which suggests fast nonradiative processes in the excited state. Consistently, the absorption spectrum of the jet-cooled acetylacetone, deduced from the photofragment excitation (PHOFEX) spectrum which monitors the LIF signal of the OH fragment as a function of the excitation energy, has been found to show no distinct structure even in the energy region near the origin.[20] Therefore, the C–O bond dissociation of the enolic acetylacetone may take place on the lower electronic states following fast nonradiative processes such as internal conversion or intersystem crossing.

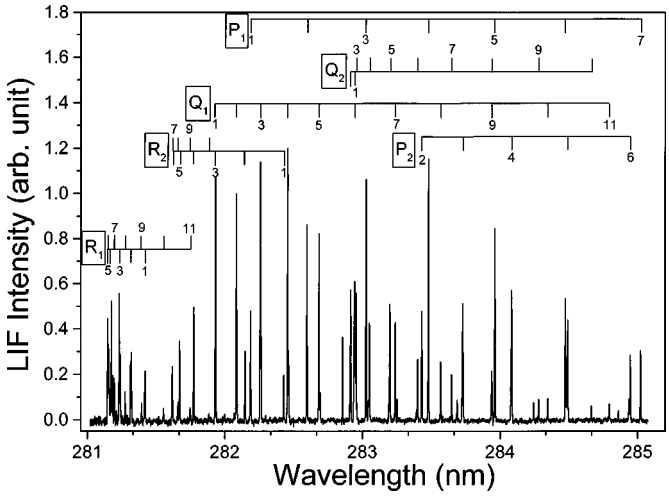

FIG. 1. A typical LIF spectrum of the OH fragment using the $A\,^2\Sigma^+$ ($v=1$)$-X\,^2\Pi$ ($v=0$) transition. The pump wavelength is 266 nm. Assignments of the bands are from Ref. 21.

The $A\,^2\Sigma^+$ ($v'=1$)$-X\,^2\Pi$ ($v''=0$) transition of OH is used for the LIF measurement. A typical LIF spectrum of the OH fragment from the acetylacetone photodissociation at 266 nm is shown in Fig. 1 with appropriate assignments for the observed peaks.[21] The OH transitions are labeled according to Hund's case (b). The *P*, *Q*, or *R* branches are for the cases of $\Delta N=-1$, 0, or 1, respectively, while the subscript 1 or 2 represents $\Pi_{3/2}$ or $\Pi_{1/2}$ states, respectively. According to the parity selection rule ($+\leftrightarrow-$), the *Q* branches probe only the Π^- state, while the *P* and *R* branches are due to the Π^+ state. The relative populations of the OH fragment are determined by dividing the LIF intensities of the transitions by their corresponding Einstein absorption coefficients.[22] The detailed analysis of the quantum state distributions of the OH fragment is presented as follows.

A. OH rotational state distribution and energetics

The OH rotational state distributions at the pump wavelengths of 291 and 266 nm, are determined by analyzing *P*, *Q*, and *R* branches from the $\Pi_{3/2}$ state. The *P* and *R* branches probe the same Λ-doublet level (Π^+, A'), and the population obtained from *P* and *R* branches are averaged to give the population of the OH fragment in the $^2\Pi_{3/2}(A')$ state (Fig. 2). Meanwhile, the *Q* branch probes the other Λ-doublet level (Π^-,A''), and is used to give the OH population in the $^2\Pi_{3/2}(A'')$ state. The OH fragment is found to be vibrationally cold at both pump wavelengths. No LIF signal due to OH ($^2\Pi$, $v''=1$) is detected in the present experimental setup. The rotational state distribution of the OH fragment ($v''=0$) is peaked at $N=3-4$, and has a long tail at the higher *N* values. It is interesting to note that the distributions obtained from the *P* and *R* branches are slightly different from those obtained from the *Q* branches. This difference

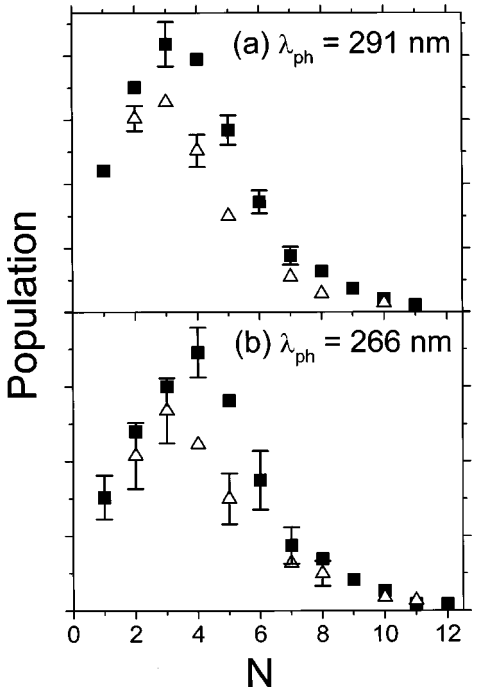

FIG. 2. OH rotational state distributions in the $^2\Pi_{3/2}(A')$state (closed rectangles) and $^2\Pi_{3/2}(A'')$ state (open triangles) at the pump wavelengths of (a) 291 and (b) 266 nm.

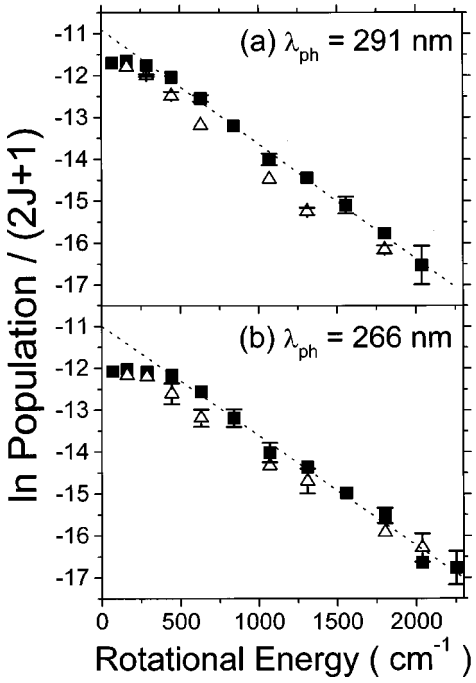

FIG. 3. Boltzmann plot of the OH rotational state distribution for the $^2\Pi_{3/2}(A')$state (closed rectangles) and $^2\Pi_{3/2}(A'')$ state (open triangles) at (a) 291 and (b) 266 nm. Non-Boltzmann behavior is observed for the low N's ($N<5$). The Boltzmann temperature obtained from the fit to the high N's ($N>5$) is $T_{rot}=530$ and 550 K for $\lambda_{ph}=291$ and 266 nm, respectively.

means that the ratio of the relative populations of the OH fragment in the Π^- and Π^+ states is not constant as a function of the rotational quantum number, and this will be discussed later (*vide infra*).

The upper bound of the available energy has been roughly estimated from the highest N value of the OH fragment of which the LIF signal is detectable at the pump wavelength of 297.5 nm (96.1 kcal/mol). The highest N value giving the detectable LIF signal is $N=10$, of which the rotational energy is 5.8 kcal/mol. Therefore, assuming that the thermal energy of the jet-cooled acetylacetone is negligible, the bond dissociation energy is less than $(96.1-5.8)=90.3$ kcal/mol. If the stabilization energy of the intramolecular hydrogen bond is taken to be 12 kcal/mol,[8] the local bond energy of the C–O(H) bond of the enolic acetylacetone would be $(90.3-12)=78.3$ kcal/mol, which is not an unreasonable value for the C–O bond energy.

The partitioning of the available energy into various degrees of freedom of fragments provides important information about the transition state involved in the photodissociation. The Boltzmann plots of the OH distribution at 291 and 266 nm are shown in Figs. 3(a) and 3(b), respectively. At the low N's, non-Boltzmann behavior is observed at both pump wavelengths, indicating that the nascent OH rotational state distribution cannot be represented by the Boltzmann rotational temperature alone. Rather, some other dynamical or more rigorous statistical models should be tried to explain the OH rotational state distribution (*vide infra*).

B. Spin–orbit state distributions

The $\Pi_{3/2}/\Pi_{1/2}$ ratios measured at 291 and 266 nm, multiplied by appropriate statistical weights, are plotted versus the OH rotational quantum number in Figs. 4(a) and 4(b), respectively. At both pump wavelengths, the $^2\Pi_{3/2}$ level seems to be slightly more populated. A spin preference has also been observed in the photodissociation of several other molecules such as NCNO,[23] HONO,[24] and NO_2.[25] However,

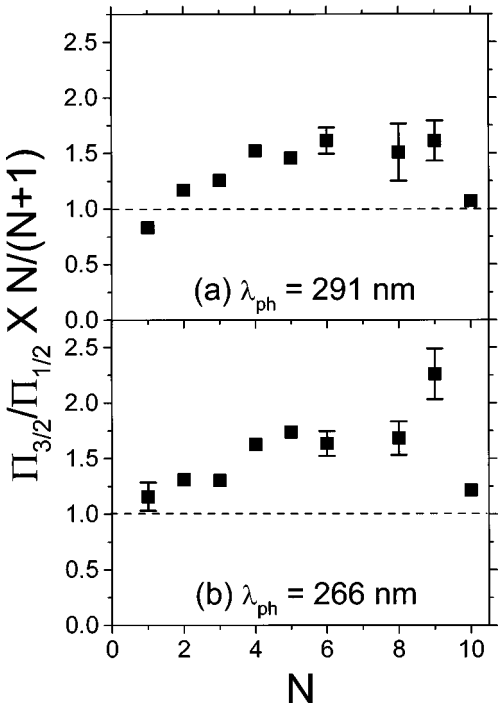

FIG. 4. Spin–orbit population ratios determined from the $^2\Pi_{3/2}(A')/^2\Pi_{1/2}(A')$ intensity ratios at (a) 291 and (b) 266 nm are plotted vs the rotational quantum number; the intensity ratios are multiplied by appropriate statistical weights.

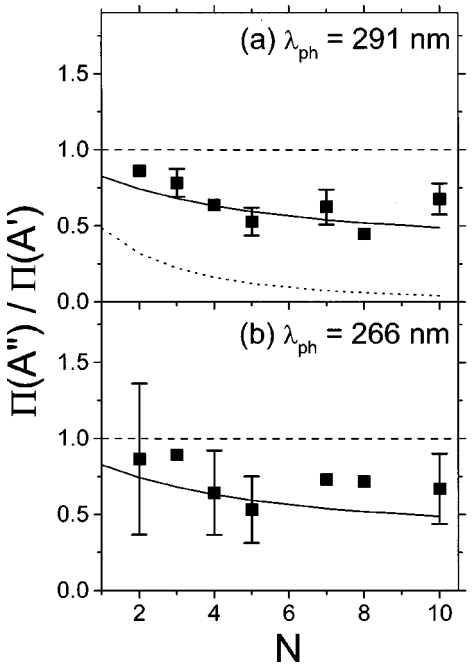

FIG. 5. Λ-doublet population ratios ($\Pi_{3/2}$) vs the OH rotational quantum number (N) at (a) 291 and (b) 266 nm. The statistical population would give unity for the Λ-doublet ratio for all N's (dashed line).

the origin of the spin preference seems to be still in debate in many cases.[23–25] It is interesting to note that since the $\Pi_{1/2}$ state lies at higher energies, the available energy for the OH fragment in the $\Pi_{1/2}$ state is lower. Therefore, the rotational state distribution is expected to be slightly shifted to the low N's for the OH fragment in the $\Pi_{1/2}$ state compared to that in the $\Pi_{3/2}$ state. This energetic difference of two spin states could be partly responsible for the slight rise of the $\Pi_{3/2}/\Pi_{1/2}$ ratio over the $N=1-6$ region in Fig. 4.

C. Population of the Λ-doublets

As mentioned earlier, the Q branches detect the OH fragment in the Π^- state, while the R (and P) branches are due to the Π^+ state.[24,26,27] Thus the Q/R (or Q/P) intensity ratios give the Λ-doublet ratios, which give information about the relative population of the OH fragment in the Π^- and Π^+ states. In the high J limit, the unpaired $p\pi$ lobe is perpendicular to the rotating plane of the OH fragment in the Π^- state (A''), while it is parallel to the rotating plane in the Π^+ state (A').[26] However, at intermediate J, the Λ-doublets are mixtures of these two limiting cases.[26]

In Figs. 5(a) and 5(b), the Λ-doublet ratios for the $\Pi_{3/2}$ state, obtained from the $Q_1/[(R_1+P_1)/2]$ ratios at 291 and 266 nm, respectively, are shown with the rotational angular quantum number. At both pump wavelengths, the Π^-/Π^+ population ratio is below unity and decreases to ~0.5 as N increases. The Π^-/Π^+ ratio represents the orientation of the $p\pi$ lobe with respect to the OH rotating plane. Therefore, the nonstatistical Λ-doublet ratios in Fig. 5 indicate that the $p\pi$ lobe containing the unpaired electron tends to be oriented in the position which is parallel to the OH rotating plane as N increases. However, the absolute value of the Π^-/Π^+ ratio is small, indicating that the $p\pi$ lobe does not reach the maximum alignment with the rotating plane even at moderately high N's.

The more quantitative analysis requires the consideration of the electronic alignment effect of the $p\pi$ lobe as OH changes from Hund's case (a) to (b) with increasing N. As first discussed by Gwinn *et al.*,[28] the orientation of the $p\pi$ lobe can be expressed in terms of $\Delta=\langle\cos^2\phi-\sin^2\phi\rangle$, where ϕ is the angle between the $p\pi$ lobe and plane of rotation. According to the analysis by Vasudev *et al.*,[24] we can extract an angle of the $p\pi$ lobe with respect to the plane of rotation from the measured Λ-doublet ratio. If the electron charge density of the $p\pi$ lobe peaks at $\phi^{\pm}$ for the $\Pi^{\pm}$ level, then

$$\phi^{\pm}=\cos^{-1}(0.5\pm|\Delta|)^{1/2}. \tag{1}$$

If θ is the angle of the $p\pi$ lobe with respect to the plane of rotation of the OH fragment, then the Λ-doublet ratio can be expressed as follows:

$$\frac{\Pi^-}{\Pi^+}=\frac{\cos^2(\phi^- -\theta)}{\cos^2(\phi^+ -\theta)}. \tag{2}$$

Suppose that the bond-breaking event occurs strictly on a molecular plane, θ will be zero, giving the dotted line in Fig. 5(a). The Λ-doublet ratios at both 291 and 266 nm are relatively well reproduced when θ is 30° [see the solid lines in Figs. 5(a) and 5(b)]. This indicates that the charge density of the $p\pi$ lobe of the OH fragment peaks at around 30° with respect to the plane of rotation, suggesting a comparatively small preference of the planar dissociation pathway.

D. Prior calculation

The partitioning of the available energy into various degrees of freedom of fragments is mainly governed by the nature of the transition state defined on the potential energy surface where the dissociation occurs.[29] In the acetylacetone dissociation, it is not clear yet which electronic states are involved in the dissociation process. One important clue for clarifying the dissociation mechanism is whether or not the product state distribution can be predictable by the statistical theory. Here, the prior model[30] is employed for the calculation of the OH rotational state distribution to be compared with the experiment.

Ab initio calculation with a 6-31+G(d) basis set on the Hartree–Fock level has been carried out for the ground state of the 3-penten-2-on-4-yl radical using the *Gaussian 98* program.[31] The 33 normal mode frequencies have been calculated. Here, it is assumed that there is no exit barrier in the dissociation and all the energetically accessible quantum states of the products are equally probable. In this case, the transition state is assumed to be located at fully separated products, and there is enough time for the energy to be randomized among all the energetically accessible quantum states of the molecule throughout the reaction pathway. Accordingly, the relative population of the OH (N) is determined by the number of quantum states of products at the energy, $E=E_{\text{aval}}-E_{\text{rot}}(\text{OH},N)$. The rotational energy of the 3-penten-2-on-4-yl radical is expected to be very low due to

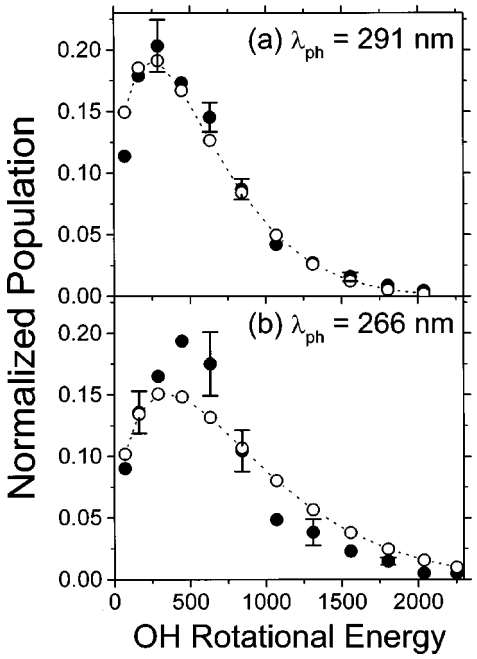

FIG. 6. The experimental OH rotational state distributions (closed circles) with prior calculations (open circles connected with dotted lines) at the photolysis wavelengths (λ_{ph}) of (a) 291 and (b) 266 nm. The experiment is well reproduced by the prior calculation in (a), while it is not in (b).

its small rotational constants ($A=0.316$ cm^{-1}, $B=0.0630$ cm^{-1}, $C=0.0387$ cm^{-1}),[31] and neglected in the prior calculation. Thus the number of vibrational quantum states of the 3-penten-2-on-4-yl radical, associated with the OH (N, $v''=0$) fragment, is counted using a Beyer–Swinehart algorithm,[32] and multiplied by the appropriate degeneracy factor $(2J+1)$ to give the calculated distribution.

The experiment and the prior calculation are compared for the OH rotational state distribution at the pump wavelength of 291 nm, Fig. 6(a). The measured OH rotational state distribution is determined by averaging over P, Q, and R branches. The overall shape of the experiment is quite well reproduced by the prior calculation. The experimental finding that the OH state distribution at 291 nm is quite well reproduced by the statistical prior model suggests that the dissociation of acetylacetone giving the OH fragment may occur on the potential energy surface without a barrier to recombination along the reaction coordinate. This means that the $\pi-\pi^*$ transition is followed by the fast internal conversion, and the OH fragment is formed via unimolecular reaction in the ground electronic state. This mechanism is quite reasonable since the recombination of two free radicals usually does not require a reaction barrier.[29]

The OH rotational state distribution at 266 nm, however, is not well reproduced by the prior calculation, Fig. 6(b). The calculation predicts the greater population at the high N's than the experiment, while at the lower N's it predicts the smaller population than the experiment. This disagreement could be simply due to the failure of the basic assumptions of the prior model at higher energies. The other possible explanation can be found in the basic concept of the variational Rice–Ramsperger–Kassel–Marcus (RRKM) theory.[33] According to the variational RRKM theory,[33] the transition state is not fixed at a specific configuration on the reaction coordinate. Rather, as the energy increases, the transition state moves along the reaction coordinate until the flux is minimized at the dynamical bottleneck. In barrierless reactions such as the singlet ketene dissociation ($^1CH_2CO \rightarrow {}^1CH_2+CO$), there has been much experimental and theoretical evidence that the transition state is loosely defined at the threshold region, but it moves in along the reaction coordinate as the energy increases above threshold.[29,34,35] Thus as the energy increases above the reaction threshold, the transition state becomes tightened, and the product state distribution cannot be described by the statistical models which count the number of the final product quantum states. Therefore, the OH rotational state distribution at 266 nm may reflect the tightened transition state at the higher energy. In this case, the variational RRKM theory[33] would be suitable to describe the product state distribution.

Even though the statistical prior model seems to describe the experiment fairly well especially at 291 nm, the possibility of the existence of the dissociation channel, which has a small exit barrier along the reaction coordinate, cannot be completely excluded. The preference of the OH fragment in the $\Pi(A')$ state (*vide supra*) indicates that the acetylacetone dissociation may not be totally statistical. If the molecule has enough time for the energy to be randomized among all the energetically accessible quantum states prior to dissociation and there is no instantaneous kicking along the exit barrier, the statistical population in the Λ-doublet states is expected. Thus the impulsive force acting along the dissociating C–O(H) bond may exist in the transition state region, giving the preferential population of the OH fragment in the $\Pi(A')$ state. In this scenario, the $\pi-\pi^*$ transition is followed by the intersystem crossing to the $^3(\pi-\pi^*)$ state, and the dissociation takes place on the triplet surface, which has an exit barrier along the reaction coordinate due to the avoided crossing with the upper electronic state (containing the σ^* character along the C–O bond) correlating to the final products. Since the impact parameter in the C–O(H) bond fragmentation is so small, the OH rotation is not expected to be highly excited even when the impulsive force along the dissociating C–O(H) bond is considerable. Furthermore, the dynamical constraint may exist in the acetylacetone dissociation due to the relatively strong intramolecular hydrogen bonding. If this is the case, the bending or internal rotation of the OH moiety coupled to the reaction coordinate could be quite asymmetric or restricted within a small range in the transition-state region. Thus the OH rotational state distribution could be only slightly different from the statistical prediction.

In order to clarify the reaction mechanism, calculations using the other various statistical models such as phase space theory (PST),[36] variational RRKM,[33] or statistical adiabatic channel model (SACM)[37] would be helpful. Experimentally, the rate constant measurement as a function of the energy and the analyses of OH Doppler profiles would be quite helpful to test various statistical or dynamical models. Eventually, *ab initio* calculation of the potential energy surfaces in the vicinity of the transition state would be desirable to investigate the role of the intramolecular hydrogen bonding

in the photodissociation of the enolic acetylacetone molecule.

IV. CONCLUSIONS

In conclusion, the enolic acetylactone gives rise to the OH fragment in the photodissociation induced by the $\pi-\pi^*$ transition. The nascent OH state distribution has been measured using the LIF technique at the pump wavelengths of 291 and 266 nm. The OH fragment is vibrationally cold, and its rotational state distribution is peaked at $N=3-4$. At the low N's, the OH rotational state distribution shows non-Boltzmann behavior. The OH fragment is found to be slightly more populated in the $^2\Pi_{3/2}$ state compared to the $^2\Pi_{1/2}$ state. The preferential population of the OH fragment in the Π^+ state is observed, and this indicates that the enolic acetylacetone may conserve the plane of symmetry throughout the reaction pathway probably due to the intramolecular hydrogen bonding.

The statistical prior model is found to be quite successful in describing the OH rotational state distribution at the pump wavelength of 291 nm, while it does not reproduce the OH rotational state distribution measured at 266 nm. This suggests that the dissociation may take place on the potential energy surface without a barrier to recombination, where the transition state is loosely defined at the threshold region and moves in along the reaction coordinate as the energy is increased. However, the existence of the dynamical constraints associated with the intramolecular hydrogen bonding should be further investigated.

ACKNOWLEDGMENTS

The authors wish to thank Professor Hong Lae Kim for helpful discussion. This work was financially supported by Korea Research Foundation made in the program year 1998–1999.

[1] T. Chiavassa, P. Verlaque, L. Pizzala, and P. Roubin, Spectrochim. Acta A **50**, 343 (1994).
[2] G. S. Hammond, W. G. Borduin, and G. A. Guter, J. Am. Chem. Soc. **81**, 4682 (1959).
[3] B. Bock, K. Flatau, H. Junge, M. Kuhr, and H. Musso, Angew. Chem. Int. Ed. Engl. **10**, 225 (1971).
[4] M. S. Gordon and R. D. Koob, J. Am. Chem. Soc. **95**, 5863 (1973).
[5] R. H. Holm and F. A. Cotton, J. Am. Chem. Soc. **80**, 5658 (1958).
[6] J. Powling and H. J. Bernstein, J. Am. Chem. Soc. **73**, 4553 (1951).
[7] H. Nakanishi, H. Morita, and S. Nagakura, Bull. Chem. Soc. Jpn. **50**, 2255 (1977).
[8] J. Dannenberg and R. Rios, J. Phys. Chem. **98**, 6714 (1994).
[9] A. H. Lowrey, C. George, P. D'Antonio, and J. Karle, J. Am. Chem. Soc. **93**, 6399 (1971).
[10] K. Iijima, A. Ohnogi, and S. Shibata, J. Mol. Struct. **156**, 111 (1987).
[11] N. S. Hush, M. K. Livett, J. B. Peel, and G. D. Willett, Aust. J. Chem. **40**, 599 (1987).
[12] R. S. Brown, J. Am. Chem. Soc. **99**, 5497 (1977).
[13] A. D. Isaacson and K. Morokuma, J. Am. Chem. Soc. **97**, 4453 (1975).
[14] C. Choi and M. M. Pintar, J. Chem. Phys. **106**, 3473 (1977).
[15] G. Karlström, B. Jönsson, B. Roos, and H. Wennerström, J. Am. Chem. Soc. **98**, 6851 (1976).
[16] X. Krokidis, V. Goncalves, A. Savin, and B. Silvi, J. Phys. Chem. A **102**, 5065 (1998).
[17] K. Hinsen and B. Roux, J. Chem. Phys. **106**, 3567 (1997).
[18] K. N. Walzl, I. M. Xavier, Jr., and A. Kuppermann, J. Chem. Phys. **86**, 6701 (1987).
[19] P. Roubin, T. Chiavassa, P. Verlaque, I. Pizzala, and H. Bodot, Chem. Phys. Lett. **175**, 655 (1990).
[20] M.-C. Yoon, Y. S. Choi, and S. K. Kim, Chem. Phys. Lett. **300**, 207 (1999).
[21] G. H. Dieke and H. M. Crosswhite, J. Quant. Spectrosc. Radiat. Transf. **2**, 97 (1962).
[22] I. L. Chidsey and D. R. Crosley, J. Quant. Spectrosc. Radiat. Transf. **23**, 187 (1980).
[23] J. Pfab, J. Häger, and W. Krieger, J. Chem. Phys. **78**, 266 (1983).
[24] R. Vasudev, R. N. Zare, and R. N. Dixon, J. Chem. Phys. **80**, 4863 (1984).
[25] H. Zacharias, M. Geihaupt, K. Meier, and K. H. Welge, J. Chem. Phys. **74**, 218 (1981).
[26] M. H. Alexander and P. J. Dagdigian, J. Chem. Phys. **80**, 4325 (1984), and references therein.
[27] P. Andresen, G. S. Ondrey, B. Titze, and E. W. Rothe, J. Chem. Phys. **80**, 2548 (1984).
[28] W. D. Gwinn, B. E. Turner, W. M. Goss, and G. L. Blackman, Astrophys. J. **179**, 789 (1973).
[29] W. H. Green, C. B. Moore, and W. F. Polik, Annu. Rev. Phys. Chem. **43**, 591 (1992).
[30] R. D. Levine and R. B. Bernstein, *Molecular Reaction Dynamics and Chemical Reactivity* (Oxford University Press, Oxford, 1987).
[31] The molecular geometry of the enolic acetylacetone in the ground state has been optimized using a 6-31G(*d*) basis set on the MP2 level, and it is assumed that the geometry of the 3-penten-2-on-4-yl radical is not changed after the dissociation.
[32] R. G. Gilbert and S. C. Smith, *Theory of Unimolecular and Recombination Reactions* (Blackwell, Oxford, 1990).
[33] D. M. Wardlaw and R. A. Marcus, Adv. Chem. Phys. **70**, 231 (1988).
[34] E. A. Wade, A. Mellinger, M. A. Hall, and C. B. Moore, J. Phys. Chem. **101**, 6568 (1997).
[35] S. W. North, D. A. Blank, J. D. Gezelter, C. A. Longfellow, and Y. T. Lee, J. Chem. Phys. **102**, 4447 (1995).
[36] P. Pechukas and J. C. Light, J. Chem. Phys. **42**, 3281 (1965).
[37] M. Quack and J. Troe, Int. Rev. Phys. Chem. **1**, 97 (1981).